RSC Advances

ROYAL SOCIETY OF CHEMISTRY

www.rsc.org/advances

Computational simulation of CO_2 removal from gas mixtures by chemical absorbents in porous membranes

Reza Fazaeli[1], Seyed Mohammad Reza Razavi[2], Mehdi Sattari Najafabadi[3], Rezvan Torkaman[4], Alireza Hemmati[1,*]

[1] Department of Chemical Engineering, Faculty of Engineering, South Tehran Branch, Islamic Azad University, P.O. Box 11365-4435, Tehran, Iran

[2] Young Researchers and Elite Club, Shahreza Branch, Islamic Azad University, Shahreza, Iran

[3] Young Researchers and Elite Club, South Tehran Branch, Islamic Azad University, Tehran, Iran

[4] Nuclear Science & Technology Research Institute, PO Box 14155-1339, Tehran, Iran

[*] Corresponding author: E-mail: alireza_hemmati@chemeng.iust.ac.ir

Abstract

In this study chemical absorption of CO_2 from N_2/CO_2 gas mixture in tetramethylammonium glycinate ($[N_{1111}]$ [Gly]) solution using hollow-fiber membrane contactors by employing CFD[1] method was investigated. A two dimensional mathematical model was developed to describe diffusion in axial and radial directions of the HFMC[2]. Also, the model gives an account of convection in the tube and the shell sides with chemical reaction between CO_2 and absorbent. Results of simulation showed good agreement with experimental data that reveals the validity of the model. CO_2 absorption from gas mixture increases as the flow rate and the concentration of

[1] Computational fluid dynamics
[2] Hollow-fiber membrane contactor

the absorbent goes up. On the other hand, increment of gas flow rate decreases removal of CO_2. The proposed model can predict CO_2 capture from gas mixtures in HFMCs.

Keywords: Membranes; Mathematical modeling; Mass transfer; CFD; Simulation; tetramethylammonium glycinate

1. Introduction

Throughout the recent years, development of industrial processes has increased the content of acid gases such as CO_2, H_2S and other sulphuric compounds in atmosphere. These compounds are released into atmosphere from burning of fossil fuels, natural gas, and industrial activities. Since carbon dioxide constitutes about 80% of greenhouse gases in atmosphere, CO_2 capture is of great importance in this regard[1]. Also, different chemical industries always take into account H_2S and CO_2 removal from gas mixtures like natural gas since CO_2 reduces efficiency of natural gas energy and H_2S is categorized as a toxic and corrosive gas[2].

Due to necessity of CO_2 capture in industries, different devices for this purpose are applied. Packed towers, spray towers, and bubble columns are typical examples of convectional industrial equipment for absorption of carbon dioxide, yet it is difficult to estimate gas-liquid mass transfer surface exactly in them and there is limited range of gas and liquid flow rates due to operational problems.

Nowadays, CO_2 removal by using gas-liquid membrane contactors has aroused great interest. A number of researchers have investigated the efficiency of membrane systems for absorption of carbon dioxide as a suitable alternative to conventional methods [3-12]. In this kind of contactor, membrane plays the role of a physical barrier between gas and liquid phases without

having any considerable effect on separation selectivity [13]. Gas-liquid membrane contactors have a high surface area per unit of contactor and due to the absence of interpenetration of two phases, they don't suffer from operational problems occurring in conventional equipment such as flooding, weeping, loading, entrainment and foaming. Other advantages of membrane systems include: smaller size, easier scaling up and scaling down, and known surface of gas-liquid interface [14]. Advantages and disadvantages of membranes have been studied by Gabelman and Hwang in more details [15].

Hollow-fiber membrane contactors (HFMCs) are being studied more than other membrane geometries because of their higher surface/volume ratio [13]. In gas-liquid absorption by HFMCs, the driving force is concentration gradient whereas the driving force is pressure gradient for systems which employ these contactors for filtration (like microfiltration). In recent years, a large number of researchers have tried to improve performance of membrane contactors for removal of CO_2 and H_2S from gas mixtures. Different parameters such as variation of liquid absorbents and their concentration, membrane materials, membrane modules, and gas and liquid flow rates were investigated in their studies [5-11, 16-41].

Membranes could provide thermal and chemical stability, and fouling and plugging problems should be kept to minimum. Furthermore, on the basis of chosen liquid absorbent, wettability should be considered for better understanding the mechanism of separation. Porous membranes are of greater interest compared with nonporous membranes since the latter have a higher penetration resistance. Nevertheless, their selectivity for carbon dioxide can be more than porous membranes [42,43]. Polysulfone (PS), polyethersulfone (PES), polyethylene (PE), polytetrafluoroethylene (PTFE), polypropylene (PP) and poly (vinylidene fluoride) (PVDF) are

examples of common hollow-fiber membranes in gas-liquid contactors, of which PP, PE and PTFE are the most conventional materials [14].

As the first researchers utilizing porous membrane as the gas-liquid contactor, Esato and Eiseman used a polytetrafluoroethylene to oxygenize blood [45]. In the following cases, researchers have used this method for separation. Qi and Cussler evaluated non-wetted polypropylene hollow-fiber membranes for the first time to capture CO_2 while there was aqueous solution of sodium hydroxide as the liquid absorbent [3,46].

Various liquid absorbents have been taken into consideration for acid-gas removal from gas mixtures by membrane processes (e.g. aqueous solutions of NaOH, KOH, NH_3, Na_2SO_3, Na_2CO_3, K_2CO_3, amines and amino acid salts). MEA, DEA, MDEA, TEA, AMP, DGA and DIPA are instances of amine solutions. Selection of liquid absorbent is affected by high reactivity with CO_2, surface tension, good thermal stability, low vapor pressure and ease of regeneration [44].

Lu et al. added AMP and piperazine as activators to methyldiethanolamine (MDEA) solution and applied it to remove carbon dioxide from CO_2/N_2 gas mixture [47]. In the other study, Ren et al. used PVDF for absorption of CO_2 [48]. Kreulen et al. put emphasis on physical and chemical removal of CO_2 by HFMCs. They studied carbon dioxide absorption in aqueous solution of glycerol by using PP membrane [49]. Dubois and Thomas evaluated performance of different absorbents including MEA, MDEA, AMP, PZ and PZEA in CO_2 capture. As they indicated, mixture of different amines improved carbon dioxide absorption efficiencies [50].

Simulation of membrane process and application of results for industrial-unit design can have a considerable consequence on reduction of costs. Some researchers have simulated

HFMCs [51-57]. Faiz *and* Al-Marzouqi theoretically studied hollow-fiber membrane contactors for CO_2 and H_2S capture by using MEA liquid absorbent and developed a 2D mass transfer model [2]. Their model combined mass transfer along with chemical reaction. Kieffer et al. have simulated mass transfer phenomena in a liquid-liquid membrane system for laminar condition [58]. They used finite element methods for simulation of process and appropriate results were obtained. Sohrabi et al. used finite element method to develop a 2D mathematical model for CO_2 absorption in amine aqueous solutions (MEA, DEA, MDEA and AMP) and potassium carbonate [59]. As their findings revealed, amines have a better performance for carbon dioxide capture as compared with K_2CO_3, due to the fact that CO_2 have a higher reaction rate and solubility with amine absorbents.

Nevertheless, amine solutions have some drawbacks such as high regeneration energy, and solvent loss, due to volatility and corrosion. Researchers try to find better substitutes such as ionic liquids (ILs) for alkanolamines. Amino-functionalized ILs are considered as good alternatives for CO_2 removal because they have high thermal stability. Ease of regeneration, non-volatility and tunable physicochemical properties are some other advantages of these absorbents [60-62]. Tetramethylammonium glycinate ($[N_{1111}][Gly]$) is an amino acid-based ionic liquid which shows a high capacity in removal of carbon dioxide in membrane processes [63,64].

Jing et al. examined the followings: density, viscosity and PH of $[N_{1111}][Gly]$, aqueous solution in concentration span of 5% to 30% of the absorbent and temperatures from 298 K to 323 K for CO_2 capture. Their findings demonstrated that removal of carbon dioxide in absorbent solution can be described by the fast pseudo-first order reaction regime. Increase in $[N_{1111}][Gly]$ concentration and CO_2 concentration would lead to increment of carbon dioxide absorption rate. On the contrary, CO_2 load shows a decrement [64].

Due to the advantages of membrane processes accompanied by the advantages of tetramethylammonium glycinate absorbent, the present study develops a 2D mathematical model for CO_2 separation from N_2/CO_2 gas mixture by [N1111] [Gly] in HFMC. Also, it investigates the effects of different parameters on the performance of the HFMC.

2. Mass transfer model

Carbon dioxide capture from N_2/CO_2 gas mixture is simulated using a 2D mass transfer model considering a hollow-fiber membrane as contactor. Fig. 1 shows a HFMC schematically. There are 21 fibers in a module which is 16 mm in outer diameter. The fibers have an outer and inner diameter of 2.2 mm and 1.4 mm, respectively. All geometrical details of the simulated HFMC are listed in Table 1 [65]. Gas mixture flows into the tube from top of the module with a flow rate of 200-1200 cm^3/min and liquid absorbent enters into the shell from the bottom side with a concentration of 15% wt. $[N_{1111}][Gly]$ and a flow rate of 50-120 cm^3/min.

Fig. 1: A schematic diagram for the hollow-fiber membrane contactor.

Table 1: Characteristics of the membrane contactor used in the simulations.

2.1. Model equation

Velocity profile in the tube side can be obtained from the Navier-Stokes equation but velocity distribution in the tube side has been considered as follows by assuming a fully-developed Newtonian laminar flow [66]:

$$V_{z-tube} = 2u\left[1-\left(\frac{r}{r_1}\right)^2\right] \quad (1)$$

where r_1 is inner radius of fiber and u (m/s) is average velocity of stream in the tube.

It is worth noting that fiber cross-sectional area is supposed to be circle-shaped, on the basis of free surface model [67] .In all processes, and for component continuity, equation can be written as follows [66]:

$$\frac{\partial C_i}{\partial t} = -(\nabla.C_i V) - (\nabla.J_i) + R_i \quad (2)$$

where C_i (mol/m^3), t (s), V (m/s), J_i (mol m^{-2} s^{-1}), and R_i (mol m^{-3} s^{-1}) indicate the concentration, time, velocity, diffusion flux and the reaction rate of component *i* respectively. Substitution of Fick's law for J_i and steady state assumption will simplify the above equation for tube side, shell side, membrane and absorbent.

2.1.1. Tube side equations

Since there occurs no chemical reaction in tube and the convection term of mass transfer in radial direction is negligible in comparison with z-direction, Eq. 2 can be expanded as:

$$D_{CO_2-tube}\left[\frac{\partial^2 C_{CO_2-tube}}{\partial r^2} + \frac{1}{r}\frac{\partial C_{CO_2-tube}}{\partial r} + \frac{\partial^2 C_{CO_2-tube}}{\partial z^2}\right] = V_{z-tube}\frac{\partial C_{CO_2-tube}}{\partial z} \quad (3)$$

where radial and axial coordinates are shown in the equation with r and z respectively. Boundary conditions related to the tube side equation are:

At r = r_1, $C_{CO_2-tube} = C_{CO_2-membrane}$ (4)

At r = 0, $\frac{\partial C_{CO_2-tube}}{\partial r} = 0$ (5)

At z=0, convective flux (6)

At z = L, $C_{CO_2-tube} = C_{CO_2,0}$ (7)

It is worth noting that convective flux as boundary condition implies no diffusion mass transfer through the boundary.

2.1.2. Shell side equations

The equation in shell side of the HFMC is given below:

$$D_{CO_2-Shell}\left[\frac{\partial^2 C_{CO_2-Shell}}{\partial r^2}+\frac{1}{r}\frac{\partial C_{CO_2-Shell}}{\partial r}+\frac{\partial^2 C_{CO_2-Shell}}{\partial z^2}\right]=V_{z-Shell}\frac{\partial C_{CO_2-Shell}}{\partial z}-R_{CO_2} \quad (8)$$

As mentioned before, for obtaining the velocity profile in the shell, Navier-Stokes equation has to be solved [66]:

$$\begin{aligned} &-\nabla.\eta\left(\nabla V_{z-Shell}+\left(\nabla V_{z-Shell}\right)^T\right)+\rho\left(V_{z-Shell}.\nabla\right)V_{z-Shell}+\nabla p=F \\ &\nabla V_{z-Shell}=0 \end{aligned} \quad (9)$$

η, ρ, V, p are dynamic viscosity (kg m^{-1} s^{-1}), density (kg m^{-3}), velocity vector (m/s), pressure (Pa) and body force (N) respectively. Happel free surface model was employed to approximate shell radius (r_3):

$$r_3=\left(\frac{1}{1-\phi}\right)^{1/2} r_2 \quad (10)$$

where r_2 is the tube outer radius. Φ indicates volume fraction of void section which is defined as follows:

$$1-\phi=\frac{nr_2^2}{R^2} \quad (11)$$

where R^2 and n are respectively the inner radius of the modules and the number of fibers. Boundary conditions for shell are as follows:

At r = r_3, $\frac{\partial C_{CO_2-shell}}{\partial r} = 0$ (12)

At r = r_2, $C_{CO_2-shell} = C_{CO_2-membrane} \times m$ (13)

At z = 0, $C_{CO_2-shell} = 0, V_{z-shell} = V_0$ (14)

At z = L, Convective flux, p = p_{atm} (15)

where m presents CO_2 solubility in absorbent.

2.1.3. Membrane equations

CO2 transfer into the pores of the membrane is done only by the diffusion. Assumption of steady state and no reaction conditions provides the below simplified continuity equation:

$$D_{CO_2-membrane}\left[\frac{\partial^2 C_{CO_2-membrane}}{\partial r^2} + \frac{1}{r}\frac{\partial C_{CO_2-membrane}}{\partial r} + \frac{\partial^2 C_{CO_2-membrane}}{\partial z^2}\right] = 0 \quad (16)$$

Boundary conditions are required for calculating Eq. 16 can be written as follows:

At r = r_1, $C_{CO_2-membrane} = C_{CO_2-shell}$ (17)

At r = r_2, $C_{CO\,2-membrane} = \frac{C_{CO_2-shell}}{m}$ (18)

Since the membrane is porous and hydrophobic, the interface is formed at the liquid phase. Therefore, no concentration change is occurred at the interface between gas and membrane.

2.1.4. Absorbent equations

Eq. 19 shows the governed equation in the shell side for [N1111] [Gly]:

$$D_{i-shell}\left[\frac{\partial^2 C_{i-shell}}{\partial r^2} + \frac{1}{r}\frac{\partial C_{i-shell}}{\partial r} + \frac{\partial^2 C_{i-shell}}{\partial z^2}\right] = V_{z-shell}\frac{\partial C_{i-shell}}{\partial z} - R_i \quad (19)$$

R_i describes the chemical reaction between absorbent and CO_2. According to the zwitterion mechanism, carbon dioxide reacts with the absorbent with the formation of a zwitterion, subsequently deprotonated by a base present in solution [61-64]:

$$H_2N-CH_2-COO^-R^+ + CO_2 \rightarrow {}^-OCC^+H_2N-CH_2-COO^-R^+$$

$${}^-OOC^+H_2N-CH_2-COO^-R^+ + B_i \rightarrow {}^-OOCHN-CH_2-COO^-R^+ + B_iH^+$$

where B_i is the bases present in the solution which can deprotonate the zwitterions, including H_2O, OH^- and $[N_{1111}][Gly]$.

Boundary conditions of Eq. 19 are:

At r = r_3, $\frac{\partial C_{absorbent-shell}}{\partial r} = 0$ (20)

At r = r_2, $\frac{\partial C_{absorbent-shell}}{\partial r} = 0$ (21)

At z = 0, $C_{absorbent\text{-}shell} = C_{absorbent,0}$ (22)

At z = L, Convective flux (23)

2.2. Numerical procedure

The commercial finite element package of COMSOL Multiphysics version 3.5 was used to solve tube, membrane and shell side equations, by applying Finite Element Method (FEM). In addition, UMFPACK was employed as a powerful solver for symmetric problems. Accuracy of UMFPACK for membrane processes has been proved by some researchers [59,65,71,73]. Fig. 2

presents triangular mesh elements relating to examining gas transfer in the HFMC. In Fig. 2, r_1, r_2, and r_3 stand for inner radius of fiber, outer radius of fiber, and radius of free surface respectively. It should be pointed out that there were 3300 elements for whole geometry.

Fig. 2: Model domain and meshes used for simulation.

3. Results and discussion

3.1. Model validation

Respecting to the author's knowledge, there is no experimental data on CO_2 capture by hollow-fiber membranes using tetramethylammonium glycinate absorbent. So, validity of the model has been assessed on the basis of experimental findings of Su-Hsia Lin et al about CO_2 separation from N_2 in the HFMC [72]. As Fig. 3 indicates, simulation is generally accurate as compared with experimental data.

Fig. 3: Relation between reaction rate and gas flow rates (for validation of model).

3.2. Velocity distribution

Figs. 4 and 5 indicate the velocity profile in the shell of the HFMC where the liquid absorbent flows through. The velocity distribution in the shell side is approximately parabolic. Moreover, the maximum velocity occurs at the middle of the shell and the amount of velocity on two walls of the shell is zero due to no-slip condition. In Fig. 4, fully developed condition exists after short distance from entrance. Indeed, hydraulic entrance length of the HFMC is small.

Fig. 4: Velocity field in the shell side (absorbent channel) of the hollow fiber membrane contactor.

Fig. 5: Velocity profile in the shell side (absorbent channel) along the membrane length.

3.3. Concentration distribution of CO_2

Fig. 6 shows dimensionless concentration distribution for CO_2 in the tube, the membrane and the shell of the HFMC. As gas mixture flows through tube, carbon dioxide transfers to membrane because of difference of concentration [64]. Regarding to Fig. 6, at z=L where gas enters the HFMC, the concentration of CO_2 has maximum value while in the other side of the membrane and at z=0 the concentration of CO_2 is equal to zero.

Mechanism of mass transfer in the tube and the shell are diffusion and convection. Since flow is in z-direction, mass is transferred via convection. In radial direction, diffusion plays the most important role on mass transfer phenomena. Gas diffuses through the pores of the membrane to the other side. According to Fig. 6, the presence of carbon dioxide at z=L in the shell side can be seen close to the membrane wall it is due to the fact that the concentration of the absorbent decreases along the HFMC and has its minimum value in the mentioned area (see Fig. 8). Consequently, reaction of absorbent with CO_2 is lower than other zones.

Fig. 7 exhibits the vector of carbon dioxide concentration in the membrane contactor. It is clearly seen that CO_2 mass transfer flux reduces along the membrane module because of carbon dioxide capture by absorbent. Moreover, variation rate of CO_2 concentration along the contactor is significant which confirms the capability of membrane contactor in successful removal of CO_2.

Fig. 6: Dimensionless concentration distribution for CO_2 in the tube, the membrane and the shell of the HFMC.

Fig. 7: Vector of total flux for CO_2 in the membrane contactor.

3.4. Concentration distribution of the absorbent

Contour of dimensionless concentration of tramethylammonium glycinate($[N_{1111}][Gly]$) in the shell of the HFMC is illustrated in Fig. 8. The liquid absorbent flows into the shell side (enters at z=0) and reacts to CO_2 which has diffused through the membrane due to difference in concentrations of two sides. Fig. 9 shows the axial variation of tetramethylammonium glycinate concentration along the HFMC. Reduction of the absorbent concentration occurs more rapidly in the middle of the contactor length. On the other hand, $[N_{1111}][Gly]$ concentration in a short distance of the entrance of the shell does not vary considerably. Because there is no CO_2 in the tube along the mentioned length, absorbent passes this length in the shell side without any reaction to carbon dioxide.

Fig. 8: Dimensionless concentration of tramethylammonium glycinate ($[N_{1111}][Gly]$) in the shell of the HFMC.

Fig. 9: Axial variation of tetramethylammonium glycinate concentration along the HFMC.

3.5. Effects of gas and liquid flow rates on CO_2 capture

The value of absorbed CO2 is calculated by using the below equation:

$$\%CO_2 \text{ removal} = 100\frac{(v \times C)_{inlet} - (v \times C)_{Outlet}}{(v \times C)_{inlet}} = 100\left(1 - \frac{C_{outlet}}{C_{inlet}}\right) \quad (24)$$

where v (m^3/s) and C (mol/m^3) are volumetric gas flow rate and concentration respectively.

The percentage of CO_2 removal versus the liquid flow rate is indicated in Fig. 10. Increment of the liquid flow rate leads to increase of the amount of carbon dioxide removal because Reynolds number and in the following mass transfer coefficient go up. When the liquid flow rate increases more, no considerable change occurs in the absorption percentage of CO_2 from the gas mixture. So, as absorbents are expensive, this can lead to reduction of unnecessary costs.

Fig. 11 indicates impacts of gas flow rate on the amount of CO_2 capture. Increase of gas flow rate associates with decrease in absorption of carbon dioxide by [N_{1111}] [Gly]. Since the resident time of the gas mixture goes down by increment of its flow rate, less amount of CO_2 can diffuse into pores of the membrane.

Fig. 10: Percentage of CO_2 removal versus the liquid flow rate.

Fig. 11: Percentage of CO_2 removal versus the gas flow rate.

3.6. Effects of the absorbent concentration on CO_2 capture

Fig. 12 shows relationship between the concentration of [N_{1111}] [Gly] and CO_2 absorption in the shell side. Increase in the absorbent concentration results in greater removal of CO_2. Therefore, carbon dioxide in outlet gas mixture stream decreases. Indeed, increment of the absorbent would lead to increase of reaction rate between CO_2 and the absorbent that ultimately causes more captured CO_2. Then, the absorbent concentration plays key role in carbon dioxide separation.

Fig. 12: Relationship between the concentration of [N_{1111}] [Gly] and Percentage of CO_2 removal.

3.7. Comparing different absorbents according to the amount of removed CO_2

For examining the efficiency of $[N_{1111}][Gly]$ absorbent, the amount of captured CO_2 by above-mentioned absorbent and two other conventional absorbents are compared in Fig. 13. As graphs show, the percentage of CO_2 removal by the studied absorbent ($[N_{1111}][Gly]$) is close to MEA as one of the most effective CO_2 absorbents. Besides, the efficiency of $[N_{1111}][Gly]$ is higher than DEA that demonstrates great effectiveness of tetramethylammonium glycinate in CO_2 separation.

Fig. 13: Comparing different absorbents according to the amount of removed CO_2.

3.8. Effect of membrane structure on separation

Effect of membrane structure in terms of porosity to tortuosity ratio on the separation performance of membrane was also investigated. The results are shown in Fig. 14 in which the percentage removal of CO_2 versus porosity/tortuosity ratio is plotted. As it can be seen, the removal of CO_2 can increase up to 90 % when the porosity to tortuosity ratio increases from 0.1 to 0.9. This behavior could be attributed to the mass transfer resistance in the membrane pores. Increasing porosity of membrane results in reduction of mass transfer resistance in the membrane phase which in turn reduces the total mass transfer resistance for transport of CO_2 from gas phase to the absorbent.

Fig. 14: Effect of porosity to tortuosity ratio on the removal of CO_2.

3.9. Effect of membrane wetting

Effect of membrane wetting on mass transfer of CO_2 from gas phase to the liquid phase was also studied to determine the favorable operational mode. The results for two different operations i.e. wetted and non-wetted modes are indicated in Fig. 15. When the membrane is considered to be hydrophobic, the pores of membrane are wetted with the gas phase, and the liquid absorbent cannot wet the membrane pores. In this case, the diffusion coefficient of CO_2 through the membrane is higher than the case when the membrane is hydrophilic. Therefore, higher mass transfer rate and also CO_2 removal is obtained in non-wetted mode (hydrophobic membrane).

Fig. 15: Effect of membrane wetting on the removal of CO_2.

4. Conclusions

A 2D mass transfer model has been developed for studying CO_2 removal in HFMCs in which tetramethylammonium glycinate ($[N_{1111}]$ [Gly]) as the absorbent was used. The continuity equations of shell, membrane and tube were solved using Finite Element Method (FEM). As regards simulation findings, the model is appropriate for prediction of hollow-fiber membrane processes performance. Increase of flow rate and concentration of absorbent improve efficiency of membrane contactor. On the contrary, by increment of gas flow rate, the percentage absorption of CO_2 declines. The amount of removed CO_2 by $[N_{1111}]$ [Gly] is between that of DEA and MEA. Furthermore, the concentration of tetramethylammonium glycinate decreases along the HFMC mainly in the middle as it flows through the shell side.

Nomenclature

C_0	inlet concentration (mol/m^3)
C	concentration (mol/m^3)
$C_{CO2-shell}$	CO_2 concentration in the shell (mol/m^3)
$C_{CO2-tube}$	CO_2 concentration in the tube (mol/m^3)
C_i	concentration of any species (mol/m^3)
$C_{i\text{-}tube}$	concentration of any species in the tube (m^2/s)
C_{in}	absorbent concentration at the inlet (mol/m^3)
C_{inlet}	inlet concentration of CO_2 in the shell (mol/m^3)
C_{outlet}	outlet concentration of CO_2 in the shell (mol/m3)
$C_{abs-shell}$	$[N_{1111}][Gly]$ concentration (mol/m3)
C_{M0}	inlet $[N_{1111}][Gly]$ concentration (mol/m3)
D	diffusion coefficient (m^2/s)
$D_{i\text{-}membrane}$	diffusion coefficient of any species in the membrane (m2/s)
$D_{i\text{-}tube}$	diffusion coefficient of any species in the tube (m2/s)
k	reaction rate coefficient of CO_2 with absorbent (m3/mol s)
L	length of a fiber (m)
m	physical solubility (–)
n	number of fibers
P	pressure (Pa)
Q_g	gas flow rate (L/h)
Q_l	liquid flow rate (L/h)
r_1	tube inner radius (m)
r_2	tube outer radius (m)
r_3	inner shell radius (m)

r	radial coordinate (m)
R	module inner radius (m)
R_i	overall reaction rate of any species (mol/m3 s)
t	time (s)
T	temperature (K)
u	average velocity (m/s)
V	velocity in the module (m/s)
$V_{z\text{-shell}}$	z-velocity in the shell (m/s)
$V_{z\text{-tube}}$	z-velocity in the tube (m/s)
Z	axial coordinate (m)

Acknowledgements

Research council at Islamic Azad University-South Tehran Branch is highly acknowledged for the financial support of this work.

References

[1] H. Herzog, B. Eliasson, O. Kaarstad, Capturing greenhouse gases, Sci. Am. 182 (2) (2000) 72–79.

[2] R. Faiz, M. Al-Marzouqi, Mathematical modeling for the simultaneous absorption of CO_2 and H_2S using MEA in hollow fiber membrane contactors, Journal of Membrane Science 342 (2009) 269–278

[3] Z. Qi, E.L. Cussler, Micro porous hollow fibers for gas absorption. Part 1: mass transfer in the liquid, J. Membr. Sci. 23 (1985) 321–332.

[4] A.B. Shelekhim, I.N. Beckman, Gas separation processes in membrane absorbent, Journal of Membrane Science, Volume 73, Issue 1, 2 October 1992, Pages 73-85, ISSN 0376-7388, http://dx.doi.org/10.1016/0376-7388(92)80187-O.

[5] Nishikawa, N., Ishibashi, M., Ohata, H., Akutsu, N., 1995. CO_2 removal by hollow fibers gas–liquid contactor. Energy Conversion and Management 36, 415–418.

[6] Feron, P.H.M., Jansen, A.E., 1995. Capture of carbon dioxide using membrane gas absorption and reuse in the horticultural industry. Energy Conversion and Man-agement 36, 411–414.

[7] Rangwala, H.A., 1996. Absorption of carbon dioxide into aqueous solutions using hollow fiber membrane contactors. Journal of Membrane Science 112, 229–240

[8] Feron, P.H.M., Jansen, A.E., 1997. The production of carbon dioxide from flue gas by membrane gas absorption. Energy Conversion and Management 38, S93–S98.

[9] Kim, Y.S., Yang, S.M., 2000. Absorption of carbon dioxide through hollow fiber membranes using various aqueous absorbents. Separation and Purification Technology 21, 101–109.

[10] Feron, P.H.M., Jensen, A.E., 2002. CO_2separation with polyolefin membrane contac-tors and dedicated absorption liquids: performance and prospects. Separation and Purification Technology 27, 231–242.

[11] Kumar, P.S., Hagendoorn, J.A., Feron, P.H.M., Versteeg, G.F., 2002. New absorption liq-uids for the removal of $CO_2$from dilute gas streams using membrane contactors. Chemical Engineering Science 57, 1639–1651.

[12] P.S. Kumar, J.A. Hogendorn, P.H.M. Feron, G.F. Versteeg, J. Membr. Sci. 213 (2003) 231.

[13]M. Rezakazemi, Z. Niazi, M. Mirfendereski, S. Shirazian, T. Mohammadi, A. Pak, CFD simulation of natural gas sweetening in a gas–liquid hollow-fiber membrane contactor, Chemical Engineering Journal 168 (2011) 1217–1226.

[14] A. Mansourizadeh, A.F. Ismail, Hollow fiber gas–liquid membrane contactors for acid gas capture: A review, Journal of Hazardous Materials 171 (2009) 38–53.

[15] A. Gabelman, S.-T.Hwang, Hollow fiber membrane contactors, Journal of Membrane Science 159 (1999) 61–106.

[16]Kreulen, H., Smolders, C.A., Versteeg, G.F., van Swaaij, W.P.M., 1993a. Micro porous hollow fiber membrane modules as gas–liquid contactors. Part 1. Physical mass transfer processes: a specific application: mass transfer in highly viscous liquids. Journal of Membrane Science 78, 197–216.

[17]Nii, S., Takeuchi, H., 1994.Removal $CO_2$and/or SO_2 from gas streams by a membrane absorption method. Gas Separation and Purification 8, 107–114.

[18]Feron, P.H.M., Jansen, A.E., Klaasen, R., 1992. Membrane technology in carbon dioxide removal. Energy Conversion and Management 23, 421–428.

[19]Kreulen, H., Smolders, C.A., Versteeg, G.F., van Swaaij, W.P.M., 1993b. Micro porous hollow fiber membrane modules as gas–liquid contactors. Part. 2. Mass transfer with chemical reaction. Journal of Membrane Science 78, 217.

[20]Karror, S., Sirkar, K.K., 1993.Gas absorption study in micro porous hollow fiber membrane modules. Industrial and Engineering Chemistry Research 32, 674–684.

[21]Chun, M.S., Lee, K.H., 1997. Analysis on a hydrophobic hollow fiber membrane absorbent and experimental observations of CO_2 removal by enhanced absorption. Separation Science and Technology 32 (15), 2445–2466.

[22]Falk-Pederson, O., Dannstorm, H., 1997.Separation of carbon dioxide from offshore gas turbine exhaust. Energy Conversion and Management 38, S81–S86.

[23]Lee, Y., Noble, R.D., Yeon, B.Y., Park, Y.I., Lee, K.H., 2001. Analysis of CO_2removal by hollow fiber membrane contactors. Journal of Membrane Science 194, 57–67.

[24]Bhaumik, D., Majumdar, S., Sirkar, K.K., 1998.Absorption of CO_2in a transverse flow hollow fiber module having a few wraps of the fiber mat. Journal of Membrane Science 138, 77–82.

[25]Li, K., Teo, W.K., 1998. Use of permeation and absorption methods for CO_2removal in hollow fiber membrane modules. Separation and Purification Technology 13, 79–88.

[26]Mavroudi, M., Kaldis, S.P., Sakellaropoulos, G.P., 2003.Reduction of CO_2 emissions by a membrane contacting process. Fuel 82, 2153–2159

[27]Yeon, S.H., Sea, B., Park, Y.L., Lee, K.H., 2003a. Determination of mass transfer rates in PVDF and PTFE hollow fibers membranes for CO_2 absorption. Separation Science and Technology 38, 271.

[28]Dindore, V.Y., Brilman, D.W.F., Feron, P.H.M., Versteeg, G.F., 2004a. CO_2absorp-tion at elevated pressures using a hollow fiber membrane contactor. Journal of Membrane Science 235, 99–109.

[29]Dindore, V.Y., Brilman, D.W.F., Geuzebroek, F.H., Versteeg, G.F., 2004b. Membrane solvent selection for CO_2removal using membrane gas–liquid contactors. Separation and Purification Technology 40, 133–145.

[30]Wang, R., Li, D.F., Liang, D.T., 2004a. Modeling of CO_2 capture by three typical amine solutions in hollow fiber membrane contactors. Chemical Engineering and Processing 43, 849–856.

[31] Wang, R., Li, D.F., Zhou, C., Liu, M., Liang, D.T., 2004b. Impact of DEA solutions with or without CO_2 loading on porous polypropylene membranes intended for use as contactors. Journal of Membrane Science 229, 147–157.

[32]Yeon, S.H., Lee, K.S., Sea, B.K., Park, Y.I., Lee, N.H., 2005.Application of pilot-scale membrane contactor hybrid system for removal of carbon dioxide from flue gas. Journal of Membrane Science 257, 156–160.

[33]Wang, R., Zhang, H.Y., Feron, P.H.M., Liang, D.T., 2005. Influence of membrane wetting on CO_2capture in micro-porous hollow fiber membrane contactors. Separation and Purification Technology 46, 33–40.

[34]Yan, S.P., Fang, M.X., Zhang, W.F., Wang, S.Y., Zu, Z.K., Luo, Z.Y., Cen, K.F., 2007. Experimental study on the separation of $CO_2$from flue gas using hollow fiber membrane contactors without wetting. Fuel Processing Technology 88, 501–511.

[35]Zhang, H.Y., Wang, R., Liang, D.T., Tay, J.H., 2006a. Modeling and experimental study of CO_2 absorption in a hollow fiber membrane contactor. Journal of Membrane Science 279, 301–310.

[36]Zhang, H.Y., Wang, R., Liang, D.T., Tay, J.H., 2008. Theoretical and experimental studies of membrane wetting in the membrane gas–liquid contacting process for CO_2absorption. Journal of Membrane Science 308, 162–170.

[37]Bottino, A., Capannelli, G., Comite, A., Firpo, R., Felice, R.D., Pinacci, P., 2006. Separation of carbon dioxide from flue gases using membrane contactors. Desalination 200, 609–611.

[38]Bottino, A., Capannelli, G., Comite, A., Felice, R.D., Firpo, R., 2008. CO_2 removal from a gas stream by membrane contactor. Separation and Purification Technology 59, 85–90.

[39] J.M. Zheng, Y.Y. Xu, Z.K. Xu, Sep. Sci. Technol. 38 (2003) 1247.

[40] D.C. Nymeijer, B. Folkers, I. Breebaart, M.H.V. Mulder, M. Wessling, J. Appl. Polym. Sci. 92 (2004) 323.

[41] H. Matsumoto, H. Kitamura, T. Kamata, M. Ishibashi, H. Ota, N. Akutsu, J. Chem. Eng. Jpn. 28 (1995) 125.

[42] S. Nii, H. Takeuchi, K. Takahashi, J. Chem. Eng. Jpn. 25 (1992) 67.

[43] M. Teramoto, K. Nakai, N. Ohnishi, Q.F. Huang, T. Watari, H. Matsuyama, Ind. Eng. Chem. Res. 35 (1996) 538.

[44]J. L. Li, B. H. Chen, Review of CO_2absorption using chemical solvents in hollow fiber membrane contactors, Separation and Purification Technology 41 (2005) 109–122

[45] K. Esato, B. Eiseman, Experimental evaluation of Core-Tex membrane oxygenator, J. Thorac. Cardiovascular Surg. 69 (1975) 690–697.

[46]Z. Qi, E.L. Cussler, Micro porous hollow fibers for gas absorption. Part 2: mass transfer across the membrane, J. Membr. Sci. 23 (1985) 333–345.

[47] J.G. Lu, Y.F. Zheng, M.D. Cheng, L.J.Wang, Effects of activators on mass-transfer enhancement in a hollow fiber contactor using activated alkanolamine solutions, J. Membr. Sci. 289 (2007) 138–149.

[48] J. Ren, R. Wang, H.Y. Zhang, Z. Li, D.T. Liang, J.H. Tay, Effect of PVDF dope rheology on the structure of hollow fiber membranes used for CO_2capture, J.Membr. Sci. 281 (2006) 334–344.

[49] H. Kreulen, C.A. Smolders, G.F. Versteeg, W.P.M. Van Swaaij, Micro porous hollow fiber membrane modules, Ind. Eng. Chem. Res. 32 (1993) 674–684.

[50]L. Dubois, D. Thomas, Carbon dioxide absorption into aqueous amine based solvents: modeling and absorption tests, Energy Procedia 4 (2011) 1353–1360

[51] Seyed Abolfazl Miramini, S.M.R. Razavi, Mehdi Ghadiri, S.Z. Mahdavi, Sadegh Moradi, CFD simulation of acetone separation from an aqueous solution using supercritical fluid in a hollow-fiber membrane contactor, Chemical Engineering and Processing: Process Intensification, Volume 72, October 2013, Pages 130-136, ISSN 0255-2701, http://dx.doi.org/10.1016/j.cep.2013.07.005.

[52]Hoff, K.A., Juliussen, O., Pedersen, O.F., Svendsen, H.F., 2004. Modeling and experimental study of carbon dioxide absorption in aqueous alkanolamine solutions using a membrane contactor.Industrial and Engineering Chemistry Research 43, 4908–4921.

[53]Keshavarz, P., Fathikalajahi, J., Ayatollahi, S., 2008. Analysis of CO_2 separation and simulation of a partially wetted hollow fiber membrane contactor. Journal of Hazardous Materials 152, 1237–1247.

[54]Evren, V., 2000. A numerical approach to determination of mass transfer performances through partially wetted micro-porous membranes: transfer of oxygen to water. Journal of Membrane Science 175, 97–110.

[55]Gong, Y., Wang, Z., Wang, S., 2006. Experimental and simulation of CO_2removal by mixed amines in a hollow fiber membrane module. Chemical Engineering and Processing 45, 652–660.

[56]Mandal, B.P., Bandyopadhyay, S.S., 2005.Simultaneous absorption of carbon dioxide and hydrogen sulfide into aqueous blends of 2-amino-2-methyl-1-propanol and diethanolamine. Chemical Engineering Science 60, 6438–6451.

[57]Al-Marzouqi, M., El-Naas, M., Marzouk, S., Abdullatif, N., 2008. Modeling of chemical absorption of CO_2 in membrane contactors. Separation and Purification Technology 62, 499–506.

[58] R. Kieffer, C. Charcosset, F. Puel, D. Mangin, Numerical simulation of mass transfer in a liquid–liquid membrane contactor for laminar flow conditions, Computers & Chemical Engineering 32 (2008) 1325–1333.

[59] M. R. Sohrabi, A. Marjani, S. Moradi, M. Davallo, S. Shirazian, Mathematical modeling and numerical simulation of CO_2 transportthrough hollow-fiber membranes, Applied Mathematical Modelling 35 (2011) 174–188.

[60] D. Wappel, G. Gronald, R.Kalb, J. Draxler, Ionic liquids for post-combustion CO2 absorption, Int. J. Greenhouse Gas Control 4 (2010) 486–494.

[61] L.M. Galan Sanchez, G.W. Meindersma, A.B. de Haan, Kinetics of absorption of CO2 in amino-functionalized ionic liquids, Chem. Eng. J. 166 (2011)1104–1115.

[62] Y.S. Zhao, X.P. Zhang, Y.P. Zhen, H.F. Dong, G.Y. Zhao, S.J. Zeng, X. Tian, S.J. Zhang, Novel alcamines ionic liquids based solvents: preparation, characterization and applications in carbon dioxide capture, Int. J. Greenhouse Gas Control 5 (2011)367–373.

[63] F. Zhang, C.G. Fang, Y.T. Wu, Y.T. Wang, A.M. Li, Z.B. Zhang, Absorption of CO2 in the aqueous solutions of functionalized ionic liquids and MDEA, Chem. Eng. J. 160 (2010) 691–697.

[64] Guohua Jing, Lanjuan Zhou, Zuoming Zhou, Characterization and kinetics of carbon dioxide absorption into aqueous tetramethylammonium glycinate solution, Chemical Engineering Journal, Volumes 181–182, 1 February 2012, Pages 85-92, ISSN 1385-8947, http://dx.doi.org/10.1016/j.cej.2011.11.007

[65] Razavi, S. M. R., Razavi, S. M. J., Miri, T., Shirazian, S., CFD simulation of CO_2 capture from gas mixtures in nanoporous membranes by solution of 2-amino-2-methyl-1-propanol and piperazine, International Journal of Greenhouse Gas Control 15 (2013) 142–149

[66] Bird, R.B., Stewart, W.E., Lightfoot, E.N., 1960. Transport Phenomena, 2nd ed. John Wiley & Sons, New York.

[67] Happel, J., 1959. Viscous flow relative to arrays of cylinders. AIChE Journal 5,174–177.

[68] Xu, G.W., Zhang, C.F., Qin, S.J., Wang, Y.H., 1992. Kinetics study on absorption of carbon dioxide into solutions of activated methyldiethanolamine. Industrial and Engineering Chemistry Research 31, 921.

[69] Xu, G.W., Zhang, C.F., Qin, S.J., Gao, W.H., Liu, H.B., 1998. Gas–liquid equilibrium in CO_2–MDEA–H_2O system and the effect of piperazine on it.Industrial and Engineering Chemistry Research 37, 1473.

[70] Seo, D.J., Hong, W.H., 1996. Solubilities of carbon dioxide in aqueous mixtures of diethanolamine and 2-amino-2-methyl-1-propanol. Journal of Chemical and Engineering Data 41, 258.

[71] Bishnoi, S., Rochelle, G.T., 2000. Absorption of carbon dioxide into aqueous piper-azine: reaction kinetics, mass transfer and solubility. Chemical Engineering Science 55, 5531.

[72] Lin, S.-H., et al., 2008. Absorption of carbon dioxide by the absorbent composed of piperazine and 2-amino-2-methyl-1-propanol in PVDF membrane contactor. JCICE 39, 13–21.

[73] Shirazian, S., Moghadassi, A., Moradi, S., 2009. Numerical simulation of mass transfer in gas–liquid hollow fiber membrane contactors for laminar flow conditions. Simulation Modelling Practice and Theory 17, 708–718.

Figure captions:

Figure1. A schematic diagram for the hollow fiber membrane contactor

Figure2. Model domain and meshes used for simulation

Figure3. Relation between reaction rate and gas flow rates (for validation of model), liquid flow rate = 100 (cm^3/min); CO_2 inlet concentration = 15 vol. %; AMP inlet concentration = 1 (mol/lit); PZ inlet concentration= 0.2 (mol/lit); temperature = 298K.

Figure4. Velocity field in the shell side (absorbent channel) of the hollow fiber membrane contactor, Gas flow rate = 200 (L/h); liquid flow rate = 100 (L/h); CO_2 inlet concentration = 15 vol. %; $[N_{1111}][Gly]$ inlet concentration = 15 wt. %; temperature = 298K.

Figure5. Velocity profile in the shell side (absorbent channel) along the membrane length, Gas flow rate = 200 (L/h); liquid flow rate = 100 (L/h); CO_2 inlet concentration = 15 vol. %; $[N_{1111}][Gly]$ inlet concentration = 15 wt. %; temperature = 298K.

Figure6. Dimensionless concentration distribution for CO_2 in the tube, the membrane and the shell of the HFMC. Gas flow rate = 200 (L/h); liquid flow rate = 100 (L/h); CO_2 inlet concentration = 15 vol. %; $[N_{1111}][Gly]$ inlet concentration = 15 wt. %; temperature = 298K.

Fig. 7: Vector of total flux for CO_2 in the membrane contactor, Gas flow rate = 200 (L/h); liquid flow rate = 100 (L/h); CO_2 inlet concentration = 15 vol. %; $[N_{1111}][Gly]$ inlet concentration = 15 wt. %; temperature = 298K.

Figure8. Dimensionless concentration of tramethylammonium glycinate ($[N_{1111}][Gly]$) in the shell of the HFMC. Gas flow rate = 200 (L/h); liquid flow rate = 100 (L/h); CO_2 inlet concentration = 15 vol. %; $[N_{1111}][Gly]$ inlet concentration = 15 wt. %; temperature = 298K.

Figure9. Axial variation of tetramethylammonium glycinate concentration along the HFMC. Gas flow rate = 200 (L/h); liquid flow rate = 100 (L/h); CO_2 inlet concentration = 15 vol. %; $[N_{1111}]$ [Gly] inlet concentration = 15 wt. %; temperature = 298K.

Figure10. Percentage of CO_2 removal versus the liquid flow rate, Gas flow rate = 200 (L/h); CO_2 inlet concentration = 15 vol. %; $[N_{1111}][Gly]$ inlet concentration = 15 wt. %; temperature = 298K.

Figure11. Percentage of CO_2 removal versus the gas flow rate, liquid flow rate = 100 (L/h); CO_2 inlet concentration = 15 vol. %; $[N_{1111}][Gly]$ inlet concentration = 15 wt. %; temperature = 298K.

Figure12. Relationship between the concentration of $[N_{1111}]$ [Gly] and Percentage of CO_2 removal, Gas flow rate = 200 (L/h); liquid flow rate = 100 (L/h); CO_2 inlet concentration = 15 vol. %; temperature = 298K.

Figure13. Comparing different absorbents according to the amount of removed CO_2. Gas flow rate = 200 (L/h); liquid flow rate = 100 (L/h); CO_2 inlet concentration = 15 vol. %; $[N_{1111}][Gly]$ inlet concentration = 15 wt. %; temperature = 298K.

Fig. 14. Effect of porosity to tortuosity ratio on the removal of CO_2. Gas flow rate = 200 (L/h); liquid flow rate = 100 (L/h); CO_2 inlet concentration = 15 vol. %; $[N_{1111}][Gly]$ inlet concentration = 15 wt. %; temperature = 298K.

Fig. 15. Effect of membrane wetting on the removal of CO_2. Gas flow rate = 200 (L/h); CO_2 inlet concentration = 15 vol. %; $[N_{1111}][Gly]$ inlet concentration = 15 wt. %; temperature = 298K.

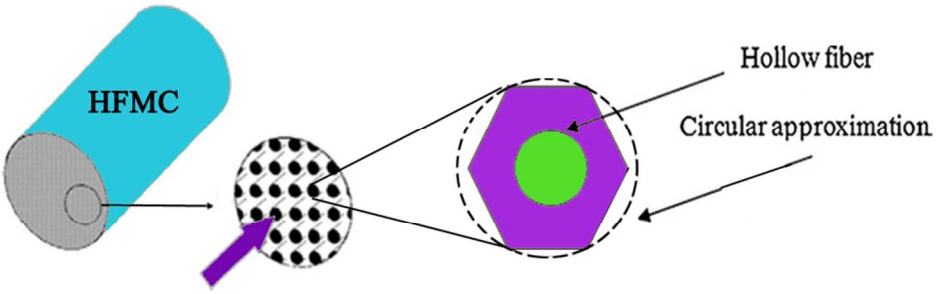

133x50mm (200 x 200 DPI)

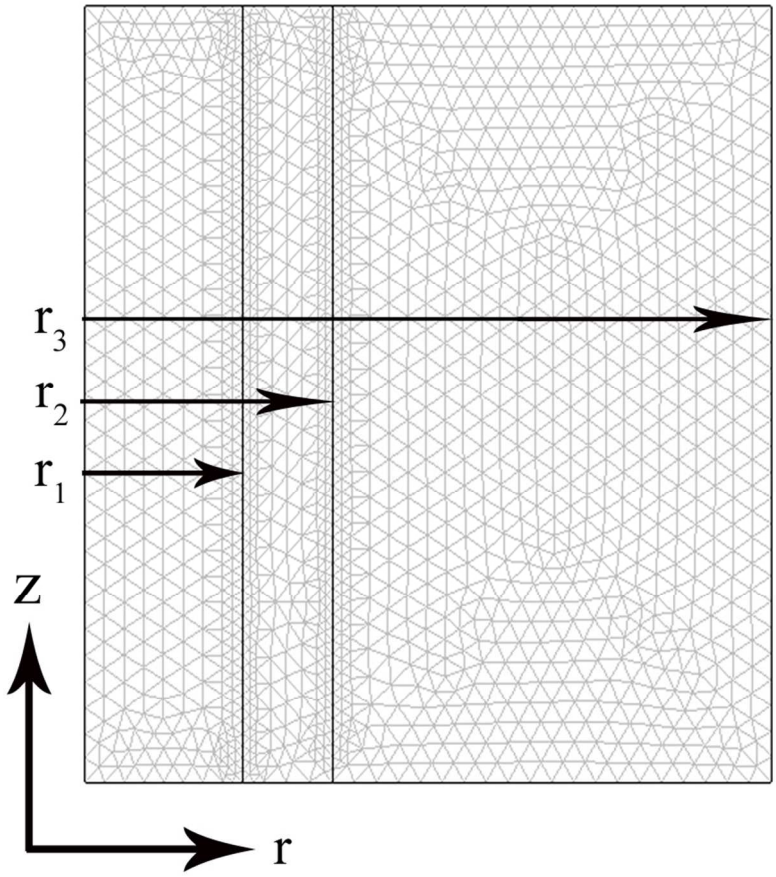

394x367mm (72 x 72 DPI)

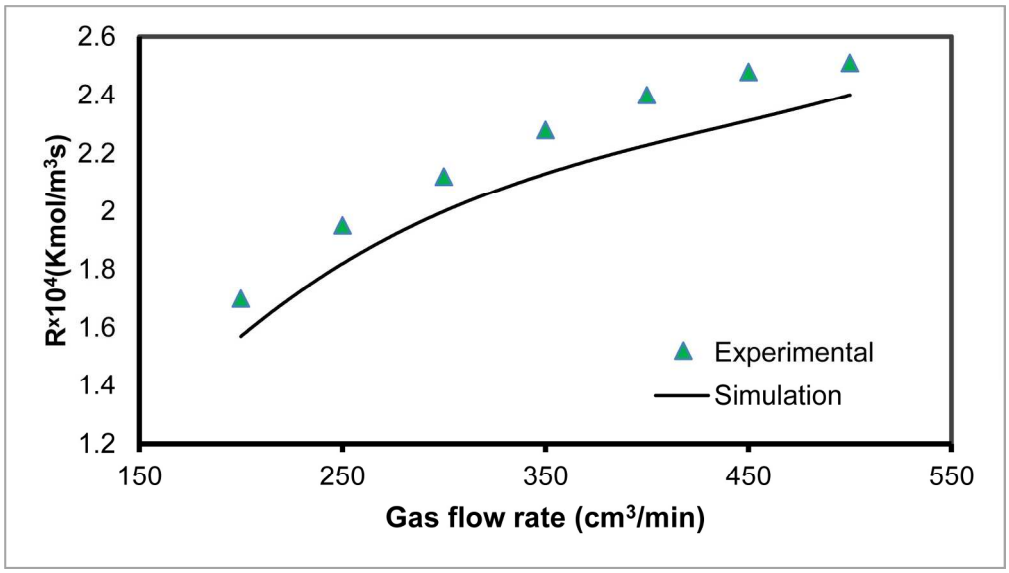

183x103mm (300 x 300 DPI)

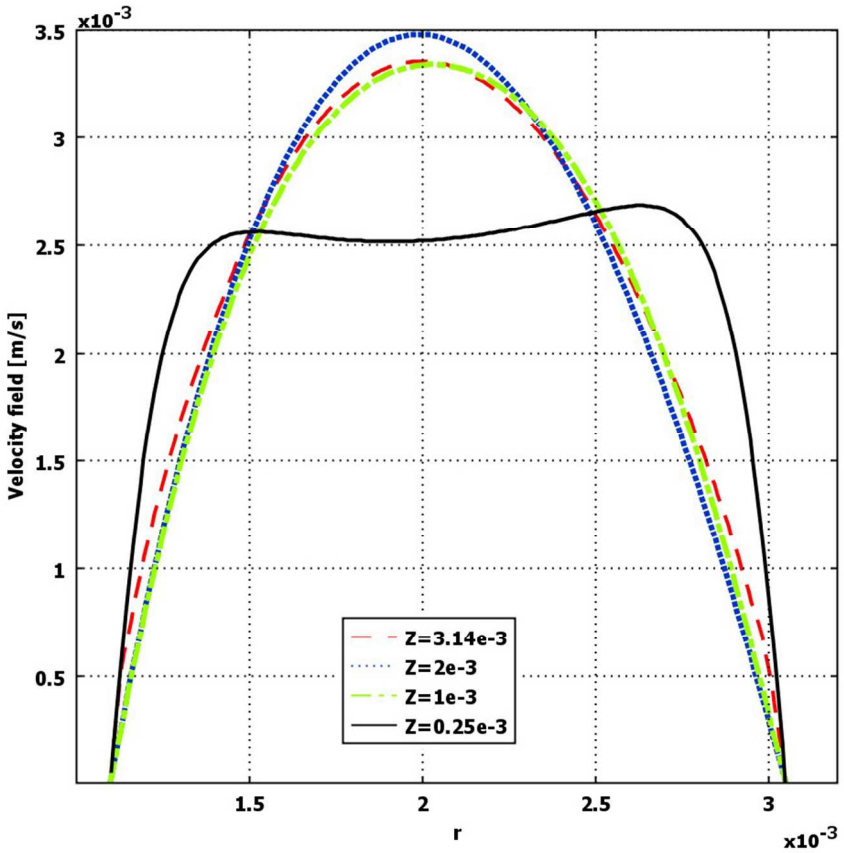

385x392mm (72 x 72 DPI)

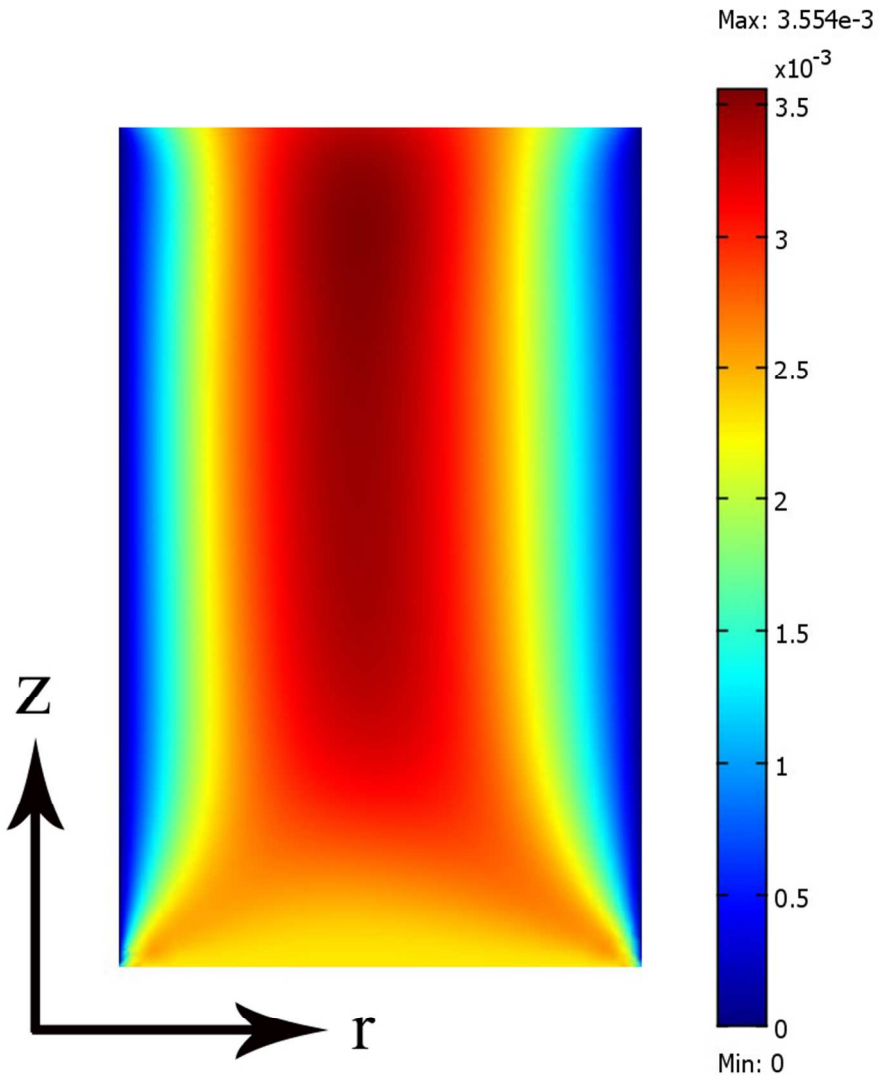

304x359mm (72 x 72 DPI)

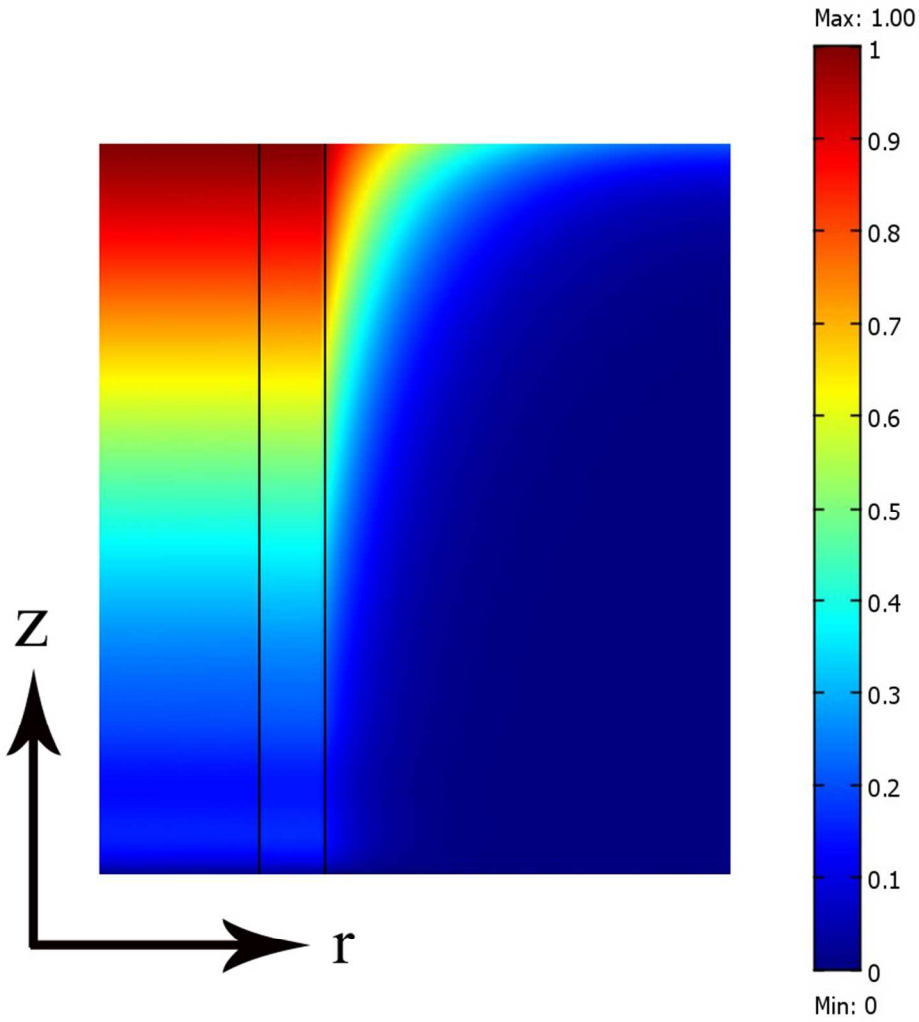

322x344mm (72 x 72 DPI)

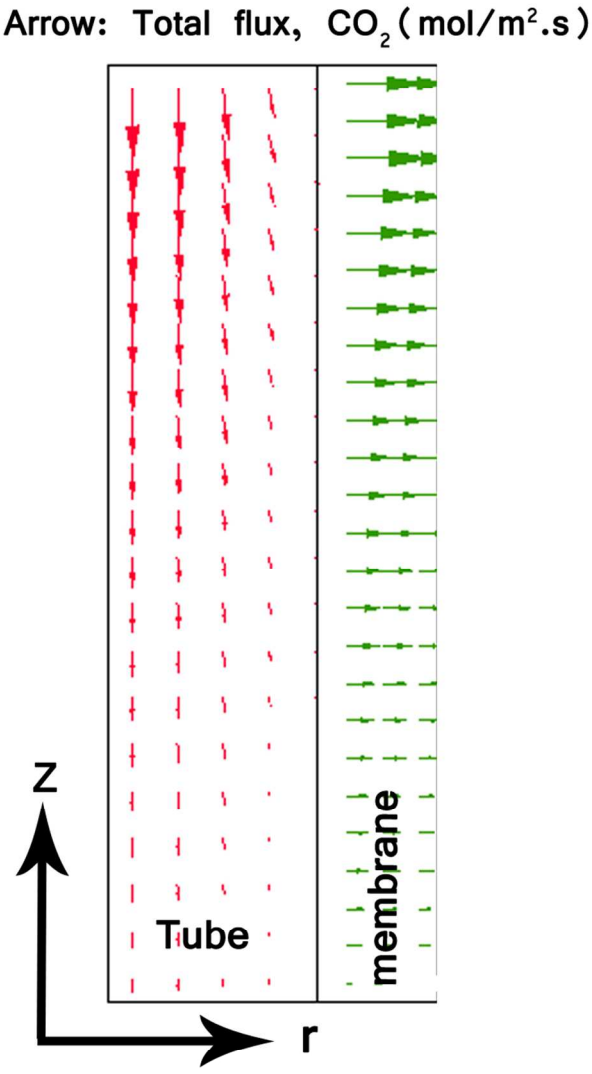

87x125mm (300 x 300 DPI)

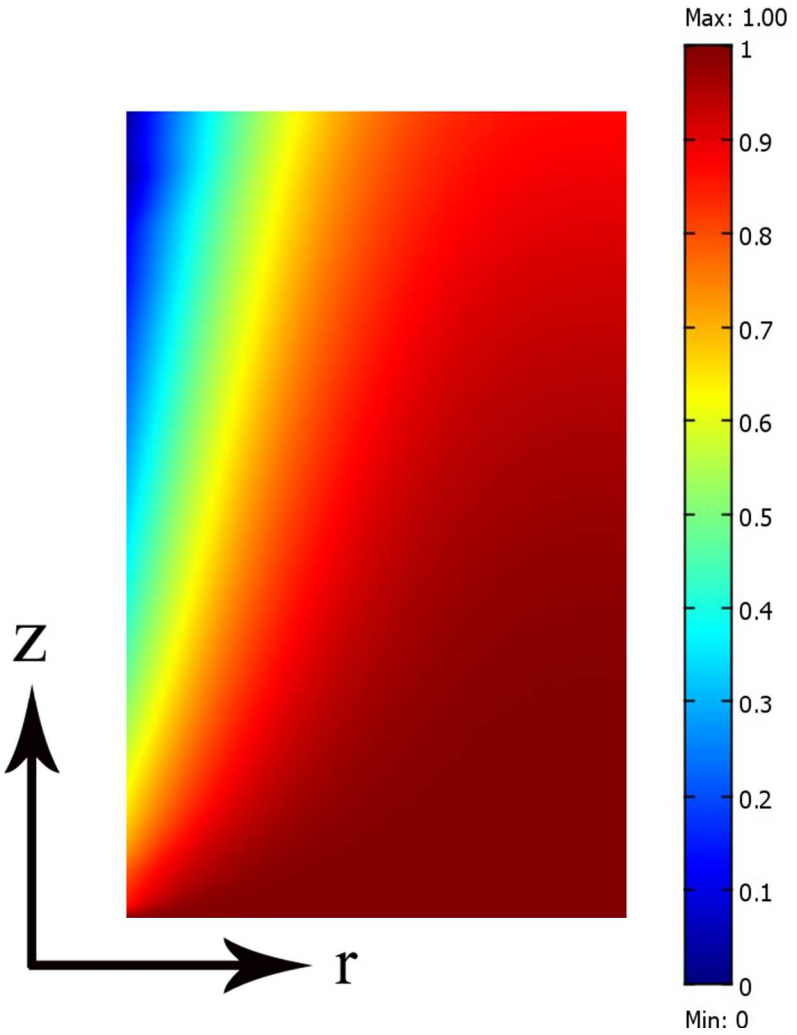

288x381mm (72 x 72 DPI)

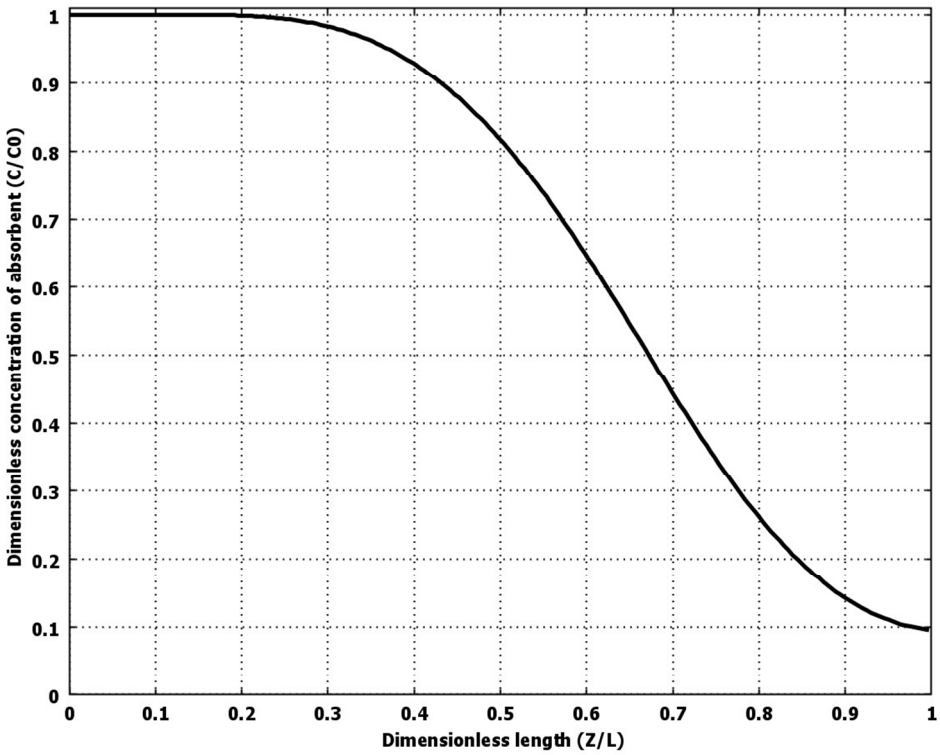

423x423mm (72 x 72 DPI)

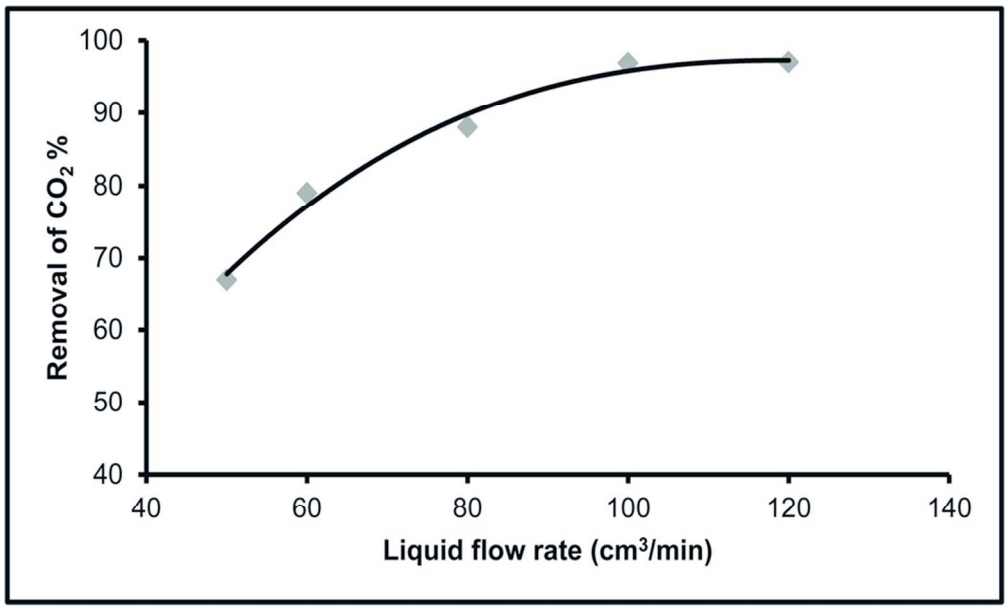

84x50mm (300 x 300 DPI)

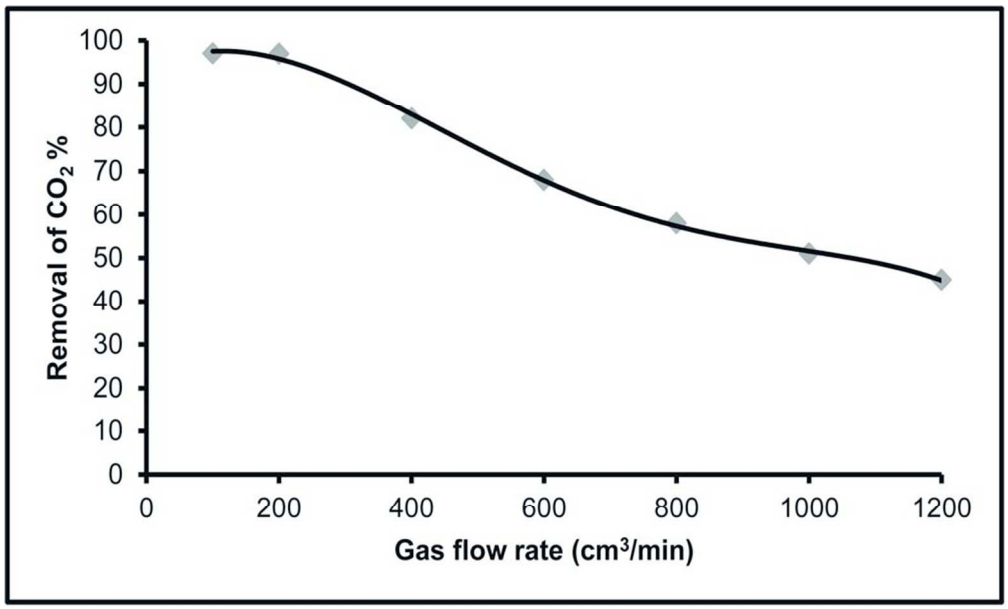

84x50mm (300 x 300 DPI)

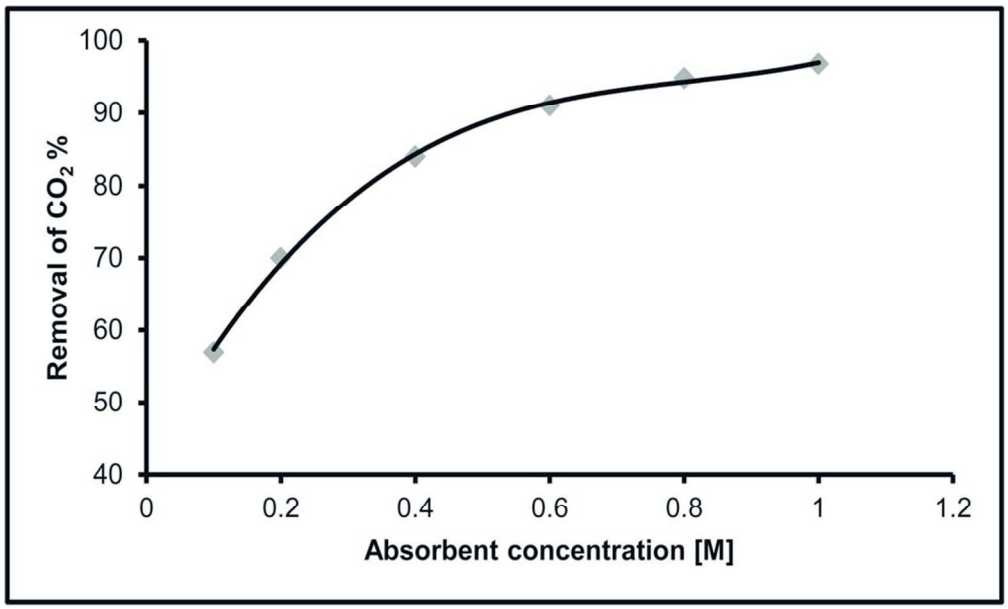

84x50mm (300 x 300 DPI)

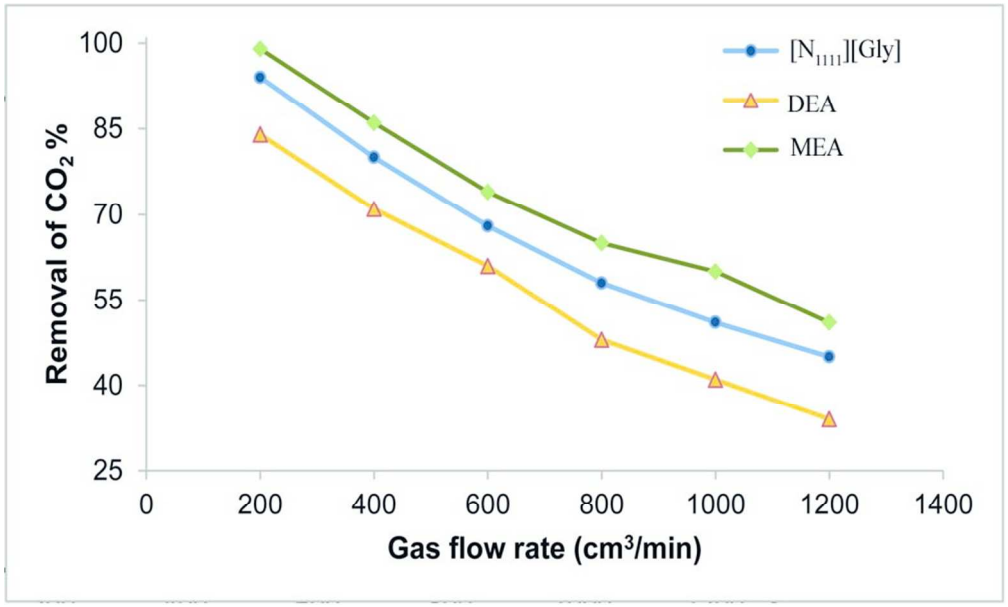

84x50mm (300 x 300 DPI)

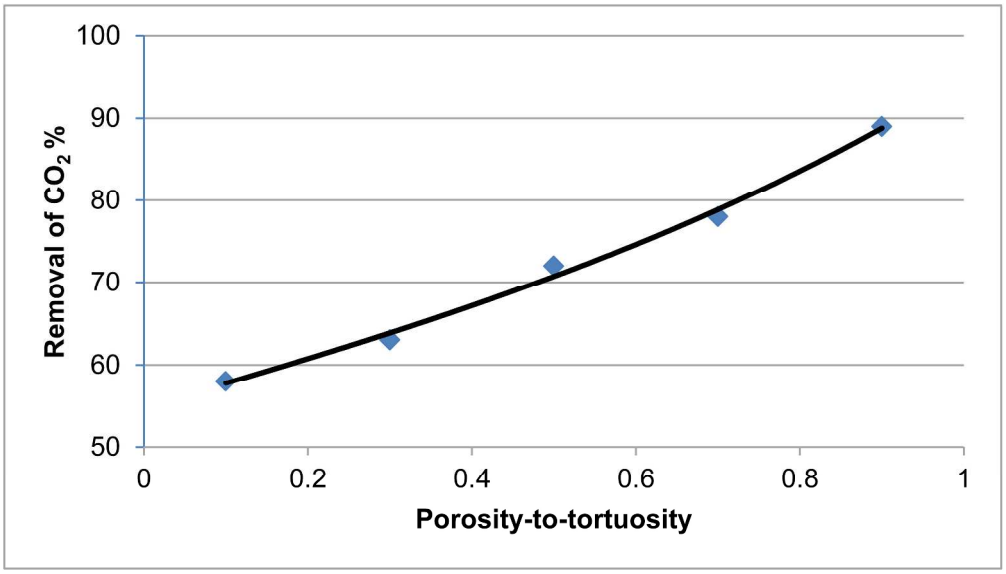

261x148mm (300 x 300 DPI)

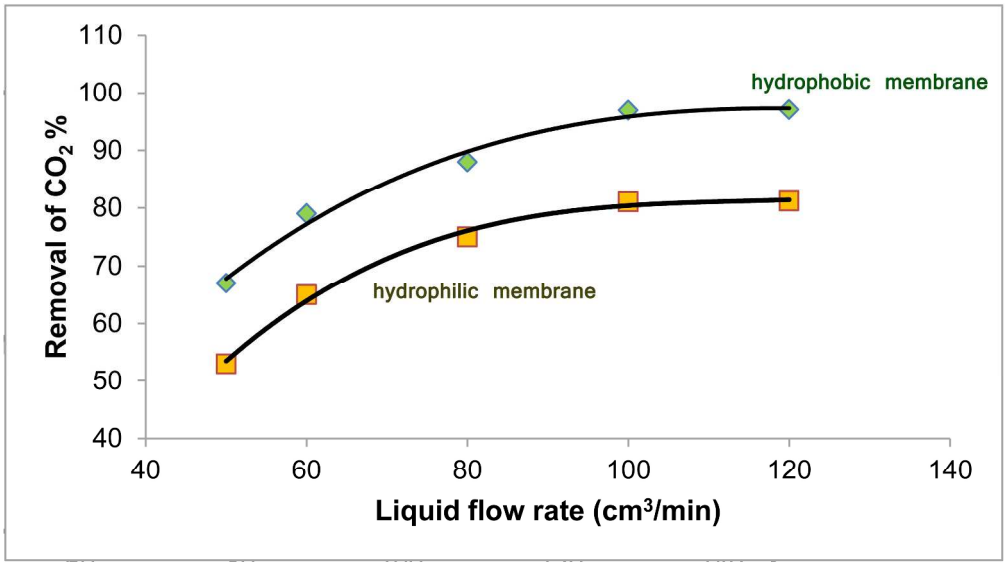

261x146mm (300 x 300 DPI)